


State of rare earth elements in the rare earth deposits of Northwest Guizhou, China

Peinan He¹ · Mingyou He²  · Hai Zhang³

Received: 28 November 2017/Revised: 19 April 2018/Accepted: 18 May 2018/Published online: 7 June 2018
© Science Press, Institute of Geochemistry, CAS and Springer-Verlag GmbH Germany, part of Springer Nature 2018

Abstract We studied the states of rare earth elements in ore of the Xianglushan rare earth deposit. Rare earth ore samples were tested and examined by scanning electron microscope, electron probe, and chemical leaching. No independent rare earth minerals were detected by scanning electron microscope. Elements detected by the electronic probe for the in situ micro-zone of the sample included: O, Al, Si, Ca, Mg, Fe, Ti, K, Na, S, Cl, C, Cu, Cr, V, and Pt. Rare earth elements were not detected by electron probe. $(\text{NH}_4)_2\text{SO}_4$, $(\text{NH}_4)\text{Cl}$, NaCl , and H_2SO_4 were used as reagents in chemical leaching experiments that easily leached out rare earth elements under the action of 10% reagent, indicating that the rare earth elements in ore are mainly in the ionic state rather than present as rare earth minerals.

Keywords Kaolinite · Clay rocks · Rare earth deposits · Element existence state · Information extraction · Northwest Guizhou Province

1 Introduction

Rare earth elements (REEs) are necessary additives in the manufacture of high-end alloy materials used for aircraft, satellites, semiconductors, special steel, and other

applications. For this reason, REEs are also called “industrial vitamins”. These important components of modern technology are not abundantly available. With the rapid development of high-end industries, REE supplies are under pressure. The search for more rare earth minerals is not only good for China’s economic development but also for industry globally.

There is a suite of kaolinite clay rocks between the top of the Permian Emeishan Basalt Formation ($\text{P}_3\beta$) and the bottom of the Xuanwei Formation (P_3x) in Weining, northwest Guizhou Province (e.g. Liu et al. 2005; Yang et al. 2005, 2008, 2010; Li et al. 2008; Pi et al. 2008; Wang et al. 2008; Zhang et al. 2008, 2016; He et al. 2013, 2014; Meng et al. 2015; Su et al. 2017). The rock is generally 3–6 m thick, with a maximum thickness of 8–10 m (Fig. 1a, b). The distribution area is over 1600 km² (He et al. 2014).

Analysis of rare earth ore samples from Lufang, Maojiaping, Zhangsigou, Xianglushan, Diaoshuiya, and Hezhang, etc. has shown total REE content (ΣREE) in ore is generally 0.2%–0.5%, with a maximum reported value of 1.086% (e.g. Wang et al. 2006; Yang et al. 2006, 2007, 2008a, b; Zhang 2014). According to geological survey data, the rare earth reserves are huge (not less than 32 million tons, calculated using a grade of 0.2%), constituting a super-large REE deposit, and inferior only to the Baiyunebo super-large REE deposits (ΣREE reserves of 36 million tons) in Inner Mongolia (Zhang 2014). The government of Guizhou Province attaches great importance to the REE resources in this area, and has set up a geological prospecting fund known as Integral exploration of iron polymetallic ores in Weining–Shuicheng area, Guizhou Province. The purpose is to quickly identify the distribution and reserves of rare earth resources, and establish a reserve base in China to alleviate the lack of rare earth

✉ Mingyou He
hmy@cdut.edu.cn

¹ College of Air Traffic Management, Civil Aviation Flight University of China, Guanghan 618307, China

² Chengdu University of Technology, Chengdu 610059, China

³ 113 Geological Team, Bureau of Geology and Mineral Resources, Liupanshui 553001, Guizhou, China

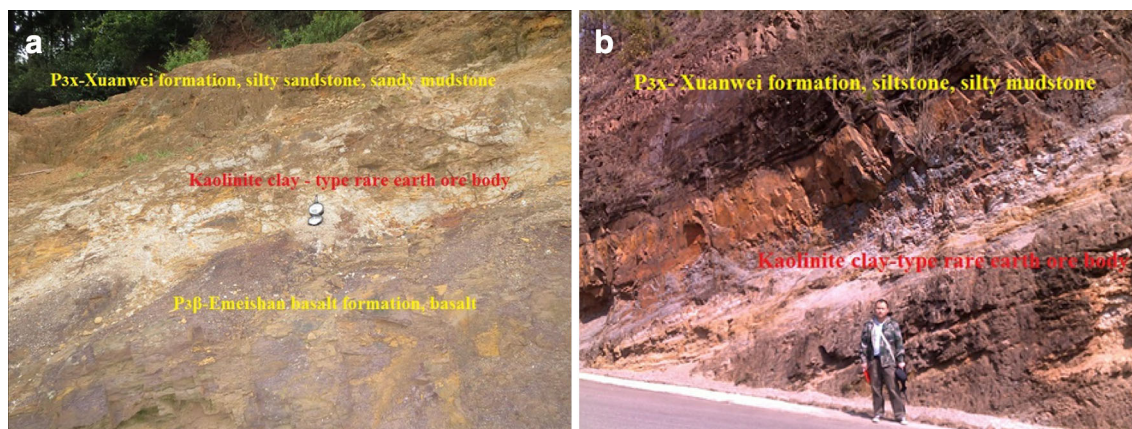


Fig. 1 **a** Close-up of landscape of rare earth ore body, **b** landscape of rare earth ore body (Highway side at the Xianglushan mine). P_{3x} -Siltstone, argillaceous sandstone, and slate; $P_{3\beta}$ -Basalt

resources in our country and around the world. REEs in this area can be extracted through industrial mining under modern technology conditions, streamlined through the study of occurrence of REEs in ore.

Some scholars believe that the REEs in Guizhou are mainly in a mineral state in florencite, bastnasite, silicon yttrium, and cerianite (Wang et al. 2006; Zhang and Dai 2010). Other scholars believe that REEs are in the ionic state and are dispersed in kaolinite clay rocks in ionic form (Zhang et al. 2013). However, in their papers, mineralogical descriptions and photo presentations of these minerals are absent. In fact, to date, no research has been carried out on the occurrence of REEs in the deposits in this area.

In this paper, presence of REEs in the Xianglushan deposit was studied.

2 Geological setting

The Xiangboshan rare earth mining area is located between Liupanshui City and Weining County in Guizhou Province. Exposed strata in the area include $P_{3\beta}$ and P_{3x} . The Xuanwei Formation and the REE-bearing series are shown in Fig. 2, with the basalt lying downsection and out of the frame.

$P_{3\beta}$ Upper purple-red volcanoclastic tuff, gray-green massive basalt, a small amount of almond-shaped basalt, columnar joints developed. The lower part is porous basalt, almond basalt, basalt tuff. Basalt and volcanoclastic tuff are rich in REEs, with ΣREE up to 223.85×10^{-6} and average content 201.98×10^{-6} (Hai Zhang 2014).

P_{3x} The upper part is lithic sandstone, siltstone, clay rock, carbonaceous shale, coal-bearing bedded siltstone; the lower part is yellowish gray siltstone, argillaceous siltstone, silty mudstone.

The REE-bearing rock series is located between $P_{3\beta}$ and P_{3x} . The deposits contain kaolinite clay type ore and iron-bearing clay type ore.

3 Sample collection

The samples were collected from two drilling holes (XZK0202 and JZK0101) and one test pit (JTC05). A total of 12 samples of rare earth ore were collected; of these, 11 were used for test analysis by Scanning Electron Microscope (SEM) and electron probe, and one for the leaching experiment. Six core samples of iron-bearing and kaolinite clay type ores were collected in borehole XZK0202. Four core samples were collected in borehole XZK0101: kaolinite clay type ore, iron-bearing clay type ore, curdle clay type ore, and silty mudstone type ore. Two ore samples of kaolinite clay type ore were collected in JTC05.

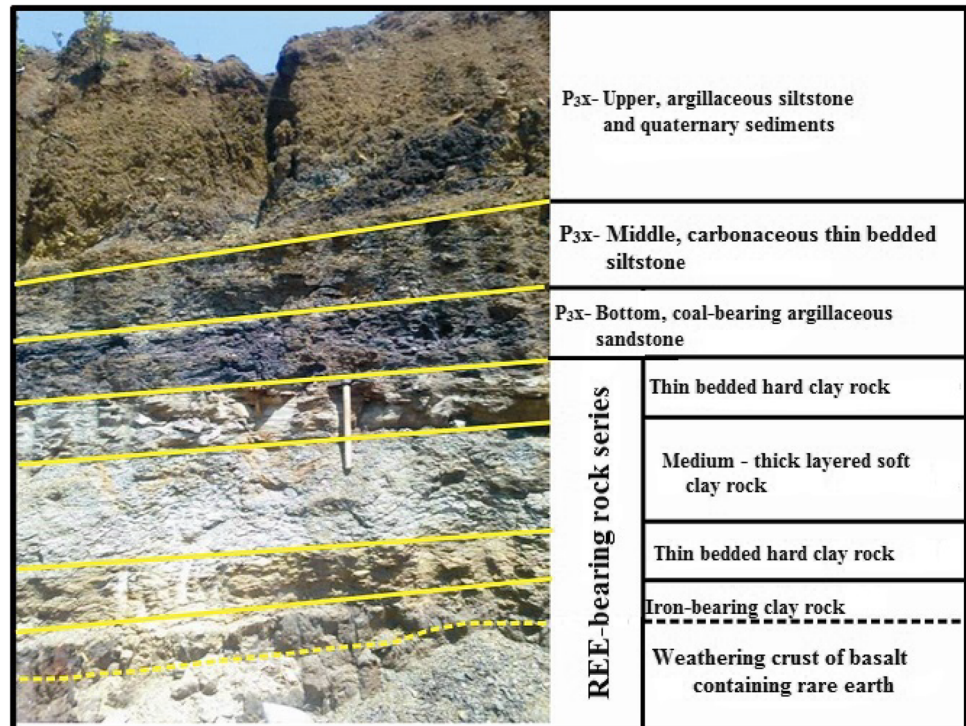
Kaolinite clay type ore: White or grayish white; muddy, layered structure. Mainly composed of clay minerals, kaolinite, hydromica(illite), montmorillonite, chlorite, and so on. The particle size of clay minerals is generally below 0.005 mm and in some cases below 0.001 mm.

Iron-bearing clay type ore: White and light red, but mainly white. Structure layout the same as kaolinite clay type ore. In addition to kaolinite, hydromica(illite), montmorillonite, and chlorite, contains a small amount of iron oxide (Fe_2O_3).

4 Analysis methods

State of REEs in samples was determined by SEM, electron probe, and experimental leaching, providing a scientific basis for judging the economic value of the rare earth

Fig. 2 Section of the rare earth element-bearing rock series in the Xianglushan area



deposits. The samples were tested and analyzed by The State Key Laboratory of Ore Deposit Geochemistry.

4.1 Instruments and equipment

SEM model: Gatan Mono CL4, Cathode Fluorescence Spectrometer (made by Gatan Company in the United States). Main technical parameters: the standard telescopic distance of the acquisition mirror is 75 mm, and the acquisition mirror thickness is 8.75 mm; the spectrometer has high efficient achromatic optical performance, can be imaged at any wavelength, and can be combined with the whole optical spectrum. The wavelength range of the detector is 185–850 nm. The sensitivity of detection of particulate matter is the nanometer scale.

EPMA model: EPMA-1600, Electron Probe-Spectrometer (made by Shimadzu Company in Japan). Performance parameters: no aberration in the crystal; acceleration voltage is 0–30 kv; resolution of the secondary electron image is ≤ 5 nm; resolution of back-scattered electron image is ≤ 20 nm; and the amplification factor is $50\times$ to $300,000\times$, continuously adjustable. Electron beam current 10–12 Å; electron beam current stability $\leq \pm 0.5 \times 10^{-3}$ /h; analysis elements range from ${}^5\text{B}$ to ${}^{92}\text{U}$; the detection limit is 10×10^{-6} .

Leaching experimental equipment: (1) Testing instrument model: HK-8100 ICP-AES (made by Beijing Huake ETS Analysis Instrument Co Ltd). Detection limit: ppb; (2) Chemical Reagents: $(\text{NH}_4)_2\text{SO}_4$, $(\text{NH}_4)\text{Cl}$, NaCl , and

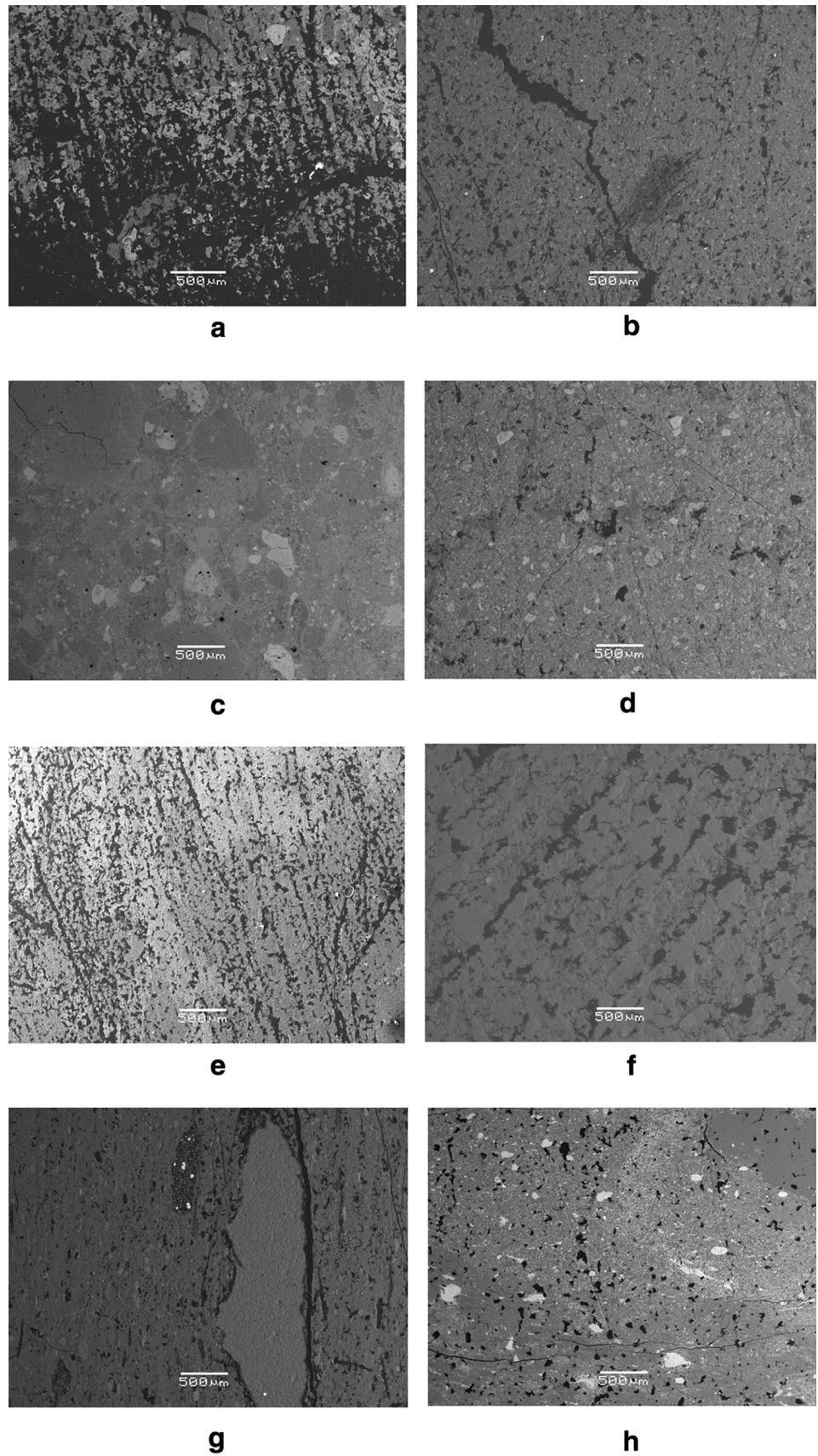
H_2SO_4 . Ammonium sulfate $(\text{NH}_4)_2\text{SO}_4$ and ammonium chloride $(\text{NH}_4)\text{Cl}$ were produced by Chengdu Ding Hengda chemical products Co. Ltd., sodium chloride (NaCl) was produced by Chengdu Hengyi chemical products Co. Ltd., and sulfuric acid (H_2SO_4) was produced by Luzhou Yizan Trade Co. Ltd.; (3) Experimental conditions: the experiment was carried out indoors under normal temperature and atmospheric pressure. Leaching time: 24 h.

4.2 Acquisition of rare earth mineral data

Data on rare earth minerals in earth ore was extracted by SEM. Eight samples were selected for SEM analysis. First, the mineral composition of the samples was observed under SEM. At the same time, minerals were selected for electron probe analysis. Then, the probe slice was sprayed with carbon and examined by SEM. SEM images of the samples are shown in Fig. 3a–h.

The SEM images show that the minerals in the rare earth ore are mainly kaolinite and clay minerals. There are also quartz, hematite, limonite, and ilmenite grains in lower numbers. Samples are fine-grained, with particle sizes mostly 10–30 μm and some up to 50 μm . Kaolinite mainly appears in a clumped distribution. Hematite, limonite, and anatase are contained in the kaolinite mass as fine particles; some are adsorbed on the surface of kaolinite and clay minerals. Rare earth minerals were not found in any of the ore samples. This does not exclude the possibility of a very small number of rare earth minerals.

Fig. 3 a XZK0202S1-1, b XZK0202S2, c XZK0202S3-1, d XZK0202S4, e JZK0101S5-1, f JZK0101S6, g JZK0101S7, h JTC05S3



4.3 The state of rare earth elements in ore

Information of REE state in rare earth ore was determined by Electron Probe Microanalysis (EPMA). The samples were analyzed by SEM, and then the locked minerals were analyzed by electron probe. Eleven rare earth ore samples were detected by EPMA, with 34 total detection points. *In-situ* micro analysis images and detection point element composition of each ore sample are shown in Figs. 4, 5, 6, 7, 8, 9, 10, 11, 12, 13 and 14.

As can be seen from the various *in situ* micro images, the selected detection points are representative, and the distribution of detection points covers all samples.

The results of 34 *in situ* micro analyses were statistically processed; detected elements were as follows: O, Al, Si, Ca, Mg, Fe, Ti, K, Na, S, Cl, C, Cu, Cr, V, and Pt—a total of 16 elements. Most are macroelements, with a small number of trace elements, namely Cu, Cr, V, and Pt.

REEs were not detected in rare earth ore samples.

A particular concern is the detection of Pt elements in the rare earth ore. In JZK0101S5-2, probe point 3 was a titanium mineral. The probe detected Pt in the titanium mineral, at 4.24 wt%. Other minerals detected included Ti (50.20 wt%), O (35.33 wt%), Al (3.79 wt%), Si (4.23 wt%), Fe (1.68 wt%), and Ca (0.53 wt%).

4.4 Leaching experiment

In order to confirm the status of rare earth elements in ore, ore of general grade was collected for chemical leaching experiments.

1. Sample description

Sampling location: The ore sample was collected from the JTC05 probe in the Xiangshan rare earth mine. Number of samples: 1. Sample Number: JTC05S. Ore type: kaolinite clay type ore. Rare earth content of the ore: 1098.6×10^{-6} . Sample weight: 3.0 kg.

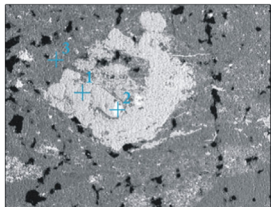
2. Experimental scheme

- (1) Sample preparation: The ore was crushed and ground into powder, to 100 mesh. Then, the sample was divided into four parts, each

weighing 500 g, and numbered: JTC05S-1, -2, -3, and -4.

- (2) Reagent: $(\text{NH}_4)_2\text{SO}_4$, $(\text{NH}_4)\text{Cl}$, NaCl, and H_2SO_4 were chosen as the leaching reagents.
 - (3) Preparation of leaching solution: The leaching solutions of $(\text{NH}_4)_2\text{SO}_4$, $(\text{NH}_4)\text{Cl}$, NaCl, and H_2SO_4 were prepared to a concentration of 10%. The volume of each leaching solution was 2.5 L.
 - (4) Leaching experiment: The samples prepared in step (1) were poured into a beaker filled with a leaching solution containing $(\text{NH}_4)_2\text{SO}_4$, $(\text{NH}_4)\text{Cl}$, NaCl, or H_2SO_4 . The solutions were stirred well for half an hour, and let stand under room temperature and atmospheric pressure. Leaching time: 24 h.
 - (5) Leaching sample preparation: After 24 h, the solution was extracted from the beakers, leaving the pulp. The pulp was then dried and leaching samples made—one for each leachate.
 - (6) Test analysis: The leaching samples were analyzed by inductively coupled plasma emission spectrometry.
3. Experimental results: experimental conditions and detection results are shown in Table 1.
- (a) When the ore samples were leached with dilute concentration reagents of $(\text{NH}_4)_2\text{SO}_4$, $(\text{NH}_4)\text{Cl}$, NaCl, and H_2SO_4 , the content of rare earth elements decreased from 1098.6×10^{-6} to: 835×10^{-6} , 972.6×10^{-6} , 983.6×10^{-6} , and 884.6×10^{-6} , respectively, indicating leaching rates of: 24.00%, 11.47%, 10.47%, and 19.48%, respectively.
 - (b) The REEs were easily extracted by the dilute reagents. This indicates a mainly ionic state of occurrence of the REEs in the ores. This does not preclude the possibility of the existence of a small amount of independent minerals or similar minerals.
 - (c) The leaching capacities of the reagents differed: $(\text{NH}_4)_2\text{SO}_4 > \text{H}_2\text{SO}_4 > (\text{NH}_4)\text{Cl} > \text{NaCl}$. The

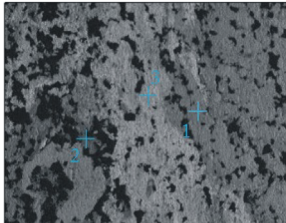
Fig. 4 Analysis results of JTC05-S3 *in situ* microregion by EPMA



Element	Wt%	At%	Element	Wt%	At%	Element	Wt%	At%
O K	35.96	56.82	S K	33.04	47.82	O K	48.85	60.77
Mg K	02.36	02.46	Cr K	01.11	00.99	Al K	22.99	13.47
Al K	13.98	13.09	Fe K	30.76	25.56	Si K	22.40	22.26
Si K	13.48	12.13	Cu K	35.09	25.63	Ti K	03.61	02.70
Fe K	34.22	15.49				Fe K	02.14	00.80
Elements of point 1			Elements of point 2			Elements of point 3		

KV 25.0 MAG 100 TILT 0.0 MICRONSPERPIX 2.450

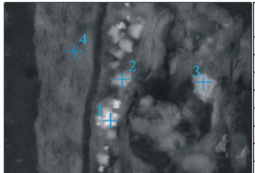
Fig. 5 Analysis results of JZK0101S5-1 in situ microregion by EPMA



Element	Wt%	At%	Element	Wt%	At%	Element	Wt%	At%
O K	38.09	56.52	O K	30.46	54.77	O K	44.67	60.15
Mg K	01.45	01.42	Al K	08.53	09.10	Al K	20.99	16.76
Al K	17.06	15.01	Si K	08.96	09.18	Si K	25.11	19.26
Si K	19.83	16.76	Ti K	01.69	01.01	Ti K	04.20	01.89
K K	00.59	00.36	Fe K	50.35	25.94	Fe K	05.04	01.94
Ca K	00.49	00.29						
Ti K	01.17	00.58						
Fe K	21.32	09.06						
Elements of point 1			Elements of point 2			Elements of point 3		

KV 25.0 MAG 100 TILT 0.0 MICRONSPERIXY 2.450

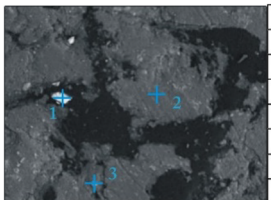
Fig. 6 Analysis results of JZK0101S5-2 in situ microregion by EPMA



Element	Wt%	At%	Element	Wt%	At%	Element	Wt%	At%	Element	Wt%	At%
O K	14.18	30.69	O K	44.08	62.44	O K	35.33	61.13	O K	44.56	59.78
Al K	03.88	04.98	Al K	03.39	02.85	Al K	03.79	03.89	Mg K	00.87	00.77
Si K	05.21	06.42	Si K	10.65	08.59	Si K	04.23	04.17	Al K	17.67	14.05
S K	26.21	28.30	P K	14.21	10.40	Pt M	04.24	00.60	Si K	28.09	21.46
Ca K	01.16	01.01	S K	00.57	00.40	Ca K	00.53	00.37	K K	01.87	01.03
Fe K	22.68	14.06	Ca K	27.09	15.32	Ti K	50.20	29.01	Ti K	03.70	01.66
Cu K	26.67	14.54				Fe K	01.68	00.83	Fe K	03.24	01.25
Elements of point 1			Elements of point 2			Elements of point 3			Elements of point 4		

KV 25.0 MAG 100 TILT 0.0 MICRONSPERIXY 2.450

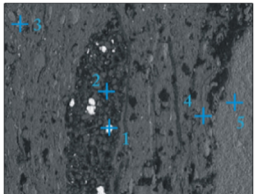
Fig. 7 Analysis results of JZK0101S6 in situ microregion by EPMA



Element	Wt%	At%	Element	Wt%	At%	Element	Wt%	At%
Si K	36.54	53.38	O K	44.89	59.08	O K	39.68	61.62
Fe K	63.46	46.62	Mg K	00.72	00.62	Al K	08.08	07.44
			Al K	23.08	18.01	Si K	10.58	09.36
			Si K	27.86	20.88	Ca K	00.58	00.36
			Ti K	01.55	00.68	Ti K	39.84	20.67
			Fe K	01.89	00.71	Fe K	01.24	00.55
Elements of point 1			Elements of point 2			Elements of point 3		

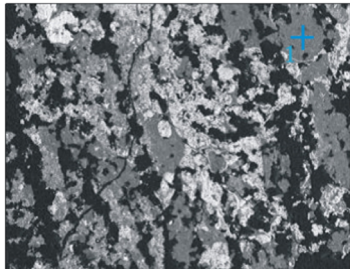
KV 25.0 MAG 300 TILT 0.0 MICRONSPERIXY 0.817

Fig. 8 Analysis results of JZK0101S7 in situ microregion by EPMA



Element	Wt%	At%	Element	Wt%	At%	Element	Wt%	At%	Element	Wt%	At%
S K	36.26	51.36	O K	42.80	65.28	O K	40.58	56.75	O K	41.27	54.87
Cr K	01.08	00.94	Al K	06.47	05.85	Mg K	01.70	01.56	Na K	10.29	09.52
Fe K	29.50	23.99	Si K	09.32	08.10	Al K	16.79	13.92	Mg K	02.95	02.58
Cu K	33.17	23.71	Ti K	36.78	18.74	Si K	27.48	21.89	Al K	00.96	00.76
Elements of point 1			Fe K	04.63	02.02	K K	00.56	00.32	Si K	38.14	28.88
O K	43.73	57.26				Ca K	00.66	00.37	Ca K	06.38	03.39
Al K	25.27	19.62				Ti K	04.36	02.04			
Si K	31.00	23.12				Fe K	07.87	03.15			
Elements of point 2			Elements of point 3			Elements of point 4			Elements of point 5		

KV 25.0 MAG 100 TILT 0.0 MICRONSPERIXY 2.450



Element	Wt%	At%
O K	44.50	59.74
Al K	20.91	16.65
Si K	26.22	20.05
Ca K	00.96	00.37
Ti K	03.66	01.64
Fe K	04.03	01.55
Elements of point 1		

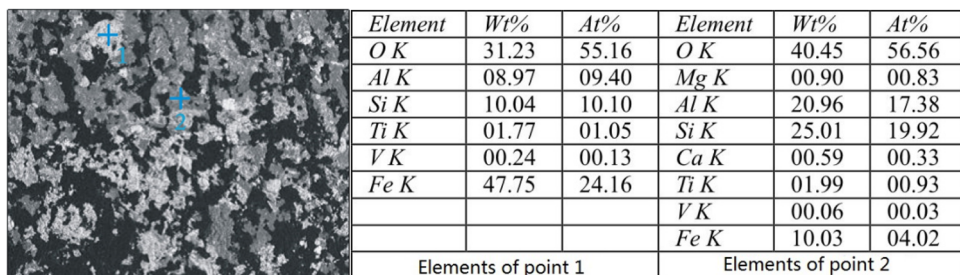
KV 25.0 MAG 100 TILT 0.0 MICRONSPERIXY 2.450

Fig. 9 Analysis results of XZK0202S1-1 in situ microregion by EPMA

leaching ability of ammonium sulfate was the strongest at 24%.

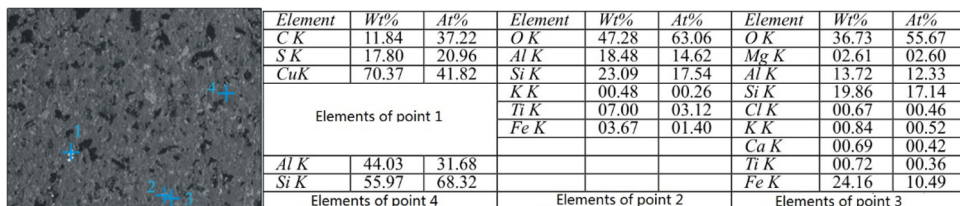
- (d) Sulfate more effectively leached the REEs than did chlorides. This is because the leaching rate is controlled by the oxidation of the reagent, and sulfates are more oxidizing than chlorides.
- (e) For the rare earth ore in northwestern Guizhou Province, $(\text{NH}_4)_2\text{SO}_4$ and H_2SO_4 are good extraction reagents, and can be used as experimental reagents for the industrial leaching of rare earth ore in the future.

Fig. 10 Analysis results of XZK0202S1-2 in situ microregion by EPMA



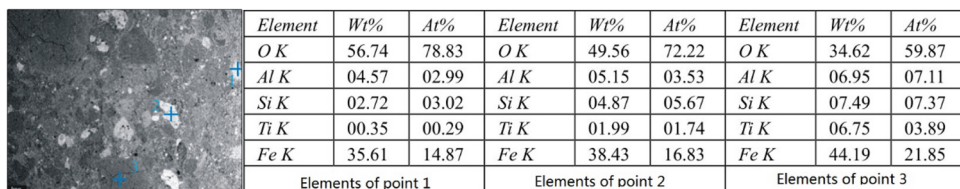
KV 25.0 MAG 100 TILT 0.0 MICRONSPERPIXIY 2.450

Fig. 11 Analysis results of XZK0202S2 in situ microregion by EPMA



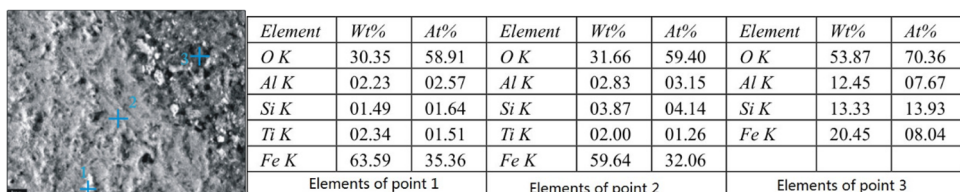
KV 25.0 MAG 100 TILT 0.0 MICRONSPERPIXIY 2.45

Fig. 12 Analysis results of XZK0202S3-1 in situ microregion by EPMA



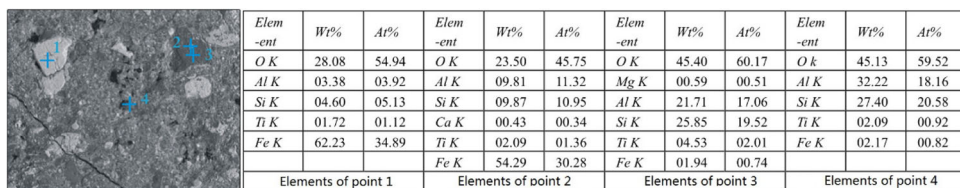
KV 25.0 MAG 30 TILT 0.0 MICRONSPERPIXIY 8.167

Fig. 13 Analysis results of XZK0202S3-2 in situ microregion by EPMA



KV 25.0 MAG 1200 TILT 0.0 MICRONSPERPIXIY 0.204

Fig. 14 Analysis results of XZK0202S4 in situ microregion by EPMA



KV 25.0 MAG 150 TILT 0.0 MICRONSPERPIXIY 1.633

Table 1 Leaching rates of the rare earth ores

Reagent	Sample	Pre-leaching (10^{-6})	Post-leaching (10^{-6})	Leaching rate (%)
(NH ₄) ₂ SO ₄	JTC05S-1	1098.6	835.0	24.00
(NH ₄)Cl	JTC05S-2	1098.6	972.6	11.47
NaCl	JTC05S-3	1098.6	983.6	10.47
H ₂ SO ₄	JTC05S-4	1098.6	884.6	19.48

5 Conclusions

Independent rare earth minerals were not detected by SEM or electron probe. However, tests showed high leaching rates of REEs from ore through dilute reagent extraction. We conclude that the REEs in the ores in northwestern Guizhou are mainly in the ionic state, not independent minerals. REE deposits in this area belong to the clay type ion adsorption deposits. This deposit is of great economic significance and is expected to become a reserve base of rare earth resources in China.

Acknowledgements This study is funded by the Guizhou Geological exploration fund (No. [2015]21) and the Guizhou Geological mineral science cooperation fund (Nos. [2015]5, [2016]5, [2017]1092).

References

- He D, Chen H, Qian L (2013) Geochemical characteristics of rare earth elements and its geological signification for mudstones of the second member of Xujiahe formation in Xinchang area. *Fault-Block Oil Gas Field* 20(2):157–161
- He M, Liu F, Zhou G, Ge W, Wang J (2014) Geological report of comprehensive survey 1:10000 for Iron polymetallic ore in Weining-Shuicheng, Guizhou Province. Chengdu University of Technology, Chengdu
- Li SJ, Xiao KH, Wo YJ, Long SX, Cai L (2008) REE geochemical characteristics and their geological signification in Silurian, west of Hunan Province and North of Guizhou Province. *Geoscience* 22(2):273–281
- Liu RE, Wei X, Wang Y, Sun FJ, Xiao HP, Zhang C (2005) The geochemical characteristics of rare earth elements of the shale rock in the geologic signification of the analysis of the sedimentary provenance: an example in the upper Palaeozoic in the Ordos basin. *Nat Gas Geosci* 16(6):788–791
- Meng C, He M, Zgang H, Guo P, Li Z, Ge W (2015) Mineralogy and petrology of iron-copper bearing strata in Weining, Northwest Guizhou. *Bull Mineral Petrol Geochem* 34(5):1058–1063
- Pi DH, Liu CQ, Deng HL, Shields G (2008) REE geochemistry of organic matter from black shales of the Niutitang formation, Zunyi, Guizhou Province. *Acta Miner Sin* 28(3):303–310
- Su H, Yang R, Gao J, Xu S, Zhang Z (2017) REE geochemical signatures and sedimentary environments of the early carboniferous Dawuba Formation Black Rock Series in Huishui, Guizhou. *J Chin Soc Rare Earths* 35(5):620–631
- Wang W, Yang R, Bao M, Wei H, Wang Q (2006) Discussion on the mineralization associated with the weathering crust on E meishan basalt in Guizhou Province China. *J Guizhou Univ (Nat Sci)* 23(4):366–370
- Wang Q, Yang R, Bao M (2008) Discussion on the role of REE in stratigraphic subdivision and correlation in coal measures from Bijie City, Guizhou Province. *Acta Sedimentol Sin* 26(1):21–27
- Yang J, Yi F, Liu T, Li H (2005) REE geochemical characters of the lower cambrian black shale series in northern Guizhou and their original significance. *Chin J Geol* 40(1):84–94
- Yang R, Wang W, Bao M, Wang Q, Wei H (2006) Geochemical characteristics of rare earth deposits at the top of Permian basalt in Hezhang Guizhou. *Min Depos* 25(A1):P205–P208
- Yang R, Bao M, Liao L, Wang W, Wei H, Wang Q (2007) Ancient weathering crust and its mineralization near the Middle-Upper Permian boundary in western Guizhou Province, China. *Acta Miner Sin* 27(1):41–47
- Yang R, Wang W, Zhang X, Liu L, Wei H, Bao M (2008a) A new type of rare earth elements deposit in weathering crust of Permian basalt in western Guizhou, NW China. *J Rare Earths* 26(5):753–759
- Yang X, Zhu M, Zhao Y, Zhang J, Guo Q (2008b) REE geochemical characteristics of the Ediacaran-Lower Cambrian black rock series in eastern Guizhou. *Geol Rev* 54(1):P3–15
- Yang G, Yu B, Chne J, Yao J, Li S, Wu Y (2010) Geochemical research on rare earth elements of argillaceous rocks of Uper-Jurassic and Cretaceous in the western Sichuan foreland basin. *Geoscience* 24(1):140–150
- Zhang H (2014) Geological and geochemical characteristics and metallogenic mechanism of REE deposits, northwestern Guizhou. Doctoral thesis. Chengdu University of Technology, pp 44–127
- Zhang Z, Dai C (2010) Rare earth ore and metallogenic geological characteristics in Guizhou. *Miner Resour Geol* 24(5):433–439
- Zhang J, Sun C, Yang G, Xie F (2008) Geochemical characteristics of REE in black shale of Lower Cambrian series of Guizhou. *Chin Rare Earths* 29(2):72–75
- Zhang H, He M, Guo P, Li Y, Zhou G (2013) Study on evolution characteristics of paleoweathering crust type iron polymetallic deposits of Permian basalts in western Guizhou. *Geol J China Univ* 19:354–355
- Zhang H, Wang Z, Wang H, Liu W (2016) REE geochemistry and sedimentary-tectonic setting of the Early Carboniferous black rock series in southern Guizhou. *Sedim Geol Tethyan Geol* 36(3):30–36